ENGINEERING JOURNAL

Article

A Maximum Likelihood Look-Ahead Unscented Rao-Blackwellised Particle Filter

Peerapol Yuvapoositanon

Centre of Electronic Systems Design and Signal Processing (CESdSP), Faculty of Engineering, Mahanakorn University of Technology, 140, Cheumsamphan Rd., Nong-Chok, Bangkok 10530, Thailand
E-mail: peerapol@mut.ac.th

Abstract. A new maximum likelihood technique for the look-ahead unscented Rao-Blackwellised particle filter (la-URBPF) to improve its robustness to noise is proposed in this paper. A radial basis function whose centre is at the state associated with the maximum likelihood is also used for masking lower likelihood states without destroying information embedded in low prior states. Simulation results show how the proposed maximum likelihood la-URBPF algorithm responds to various noise levels ranging from relatively low to aggressively high levels. The computational times for different noise levels of the proposed algorithm are also investigated to assess its applicability in time-critical or in resource-restricted embedded systems.

Keywords: Fault diagnosis, maximum likelihood, particle filters, look-ahead unscented Rao-Blackwellised particle filter.

ENGINEERING JOURNAL Volume 21 Issue 6
Received 28 August 2017
Accepted 16 October 2017
Published 31 October 2017
Online at http://www.engj.org/
DOI:10.4186/ej.2017.21.6.47

DOI:10.4186/ej.2017.21.6.47

1. Introduction

Particle filters are considered attractive for fault diagnosis mainly due to their capabilities in representing arbitrary distributions, hence making them suitable for uncertain and ever-changing worlds of autonomous vehicles and planetary robots [1]. They are also robust to noisy sensor signal acquisition and the number of particles can be compromised between accuracy and available resources of computation [1]. However, one major problem of using particle filters in fault diagnosis is that the fault states usually have very low probability to occur. So there might be no particle in a fault state when a fault occurs and the system will be unable to diagnose the fault [2]. Nevertheless, by marginalising the posterior density it is possible to select particles before the sampling step. Then, the fittest particles at time t is chosen using the information at time $t-1$ [3]. This ***look-ahead*** strategy tends to be more robust to outliers since the future information will correct the misinformation from the outliers [4]. The look-ahead strategy altogether with a technique of marginalising out some of the variables is then collectively called the look-ahead Rao–Blackwellised particle filter (la-RBPF) and is applied for fault diagnostic tasks in two industrial processes: an industrial dryer and a level-tank [3]. Also in [5], the la-RBPF is adopted for detecting faults in the autonomous operation of a mobile waiter robot and planetary rovers designed by NASA for Mars exploration. The results therein show how the la-RBPF outperforms existing particle filters in decreasing of diagnosis errors and variances especially when the number of particles is relatively low, i.e., < 100.

In [6], the look-ahead unscented Rao-Blackwellised Particle Filtering (la-URBPF) algorithm is introduced to the problem of fault diagnosis of the suspension system of the K-9 rover at NASA Ames Research Center. It proves to offer a noticeable performance gain to the existing algorithms and also lends itself to non-linear state estimation problems. A fast version of la-URBPF called Fast la-URBPF is introduced in [7] to effectively reduce the complexity of URBPF by strategically limiting the numbers of the unscented Kalman Filter (UKF) predictions and updates.

Nevertheless, la-URBPF can perform differently, if not unfavourably, in ***moderate*** to ***high*** noise scenarios. Such undesired behaviour has also been reported in problems with large number of discrete states such as the Simultaneous Localisation and Mapping (SLAM) [8]. This is mainly due to perturbation in the form of ***likelihood*** of all possible discrete states generated in the process of UKF updates. Even though in fault diagnosis problems whose number of discrete states are usually low, la-URBPF will fail miserably in high noise scenarios and the expected benefits of using la-URBPF instead of its plain URBPF counterparts is no further relevant [5], [9]. Simply increasing the number of particles (e.g., from 10 to 50) cannot improve the situation in such noisy environments [9]. A moving-average filter may be applied on the measurement data to restore the benefit of la-RBPF [5]. But this approach relies on knowledge of the specific noise level and involves a further step in designing of such filter.

In this paper, we propose a maximum likelihood technique to improve the robustness of la-URBPF for aggressively noisy fault diagnosis systems. Since the highest prior state is usually associated with the maximum likelihood, the state calculated after UKF update with the maximum likelihood is therefore selected for computing posterior probability. The other states with smaller likelihood may either be actual states with lower priors or undesired noise. Therefore, in order to suppress the noise but still retain information for states with low priors, a radial basis function whose centre is at the state associated with the maximum likelihood is used for masking lower likelihood states without destroying information embedded in low prior states.

Simulation results show how the proposed maximum likelihood la-URBPF algorithm responds to a various amount of noise ranging from relatively low to aggressively high levels. The computational times for different noise levels of the proposed algorithm are also investigated to assess its applicability in time-critical or in resource-restricted embedded systems.

Notation: We use bold lower case for both random variables and their realisation vectors. Bold upper case is for matrices. The conditional probability distribution and the conditional probability density are denoted by $P(\cdot|\cdot)$ and $p(\cdot|\cdot)$ respectively. $\boldsymbol{\theta} \sim \mathcal{N}(\boldsymbol{\mu}, \boldsymbol{\Sigma})$ denotes the distribution of normal (Gaussian) distributed with mean $\boldsymbol{\mu}$ and covariance $\boldsymbol{\Sigma}$. The conditional expectation operator is denoted

by $E\{\cdot|\cdot\}$. The notation $\boldsymbol{\theta}_{0:t}$ represents the set of variables $\boldsymbol{\theta}$ up to time t and is defined by $\boldsymbol{\theta}_{0:t} \triangleq \{\boldsymbol{\theta}_i,\ i = 0, \ldots, t\}$.

2. System Model

We consider the problem of fault diagnosis by means of a state-space system model representation [5]

$$\begin{aligned} \boldsymbol{z}_t &\sim P(\boldsymbol{z}_t|\boldsymbol{z}_{0:t-1}), \\ \boldsymbol{x}_t &= A(\boldsymbol{z}_t)\boldsymbol{x}_{t-1} + B(\boldsymbol{z}_t)\boldsymbol{w}_t + F(\boldsymbol{z}_t)\boldsymbol{u}_t, \\ \boldsymbol{y}_t &= C(\boldsymbol{z}_t)\boldsymbol{x}_t + D(\boldsymbol{z}_t)\boldsymbol{v}_t + G(\boldsymbol{z}_t)\boldsymbol{u}_t, \end{aligned} \tag{1}$$

where $\boldsymbol{y}_t \in \mathbb{R}^{n_y}$ denotes the observations or measurements, $\boldsymbol{x}_t \in \mathbb{R}^{n_x}$ the unknown Gaussian continuous states $\boldsymbol{u}_t \in \mathbb{U}$ is a known control signal, $\boldsymbol{z}_t \in \{1, ..., n_z\}$ denotes the unknown discrete states for all n_z possible states. Past to present values are denoted collectively as $\boldsymbol{z}_{0:t} \triangleq \{\boldsymbol{z}_0, \ldots, \boldsymbol{z}_t\}$, $\boldsymbol{x}_{0:t} \triangleq \{\boldsymbol{x}_0, \ldots, \boldsymbol{x}_t\}$, $\boldsymbol{y}_{1:t} \triangleq \{\boldsymbol{y}_1, \ldots, \boldsymbol{y}_t\}$ and $\boldsymbol{u}_{1:t} \triangleq \{\boldsymbol{u}_1, \ldots, \boldsymbol{u}_t\}$. The noise processes are iid Gaussian with $\boldsymbol{w} \sim \mathcal{N}(0, I)$ and $\boldsymbol{v}_t \sim \mathcal{N}(0, I)$.

3. The Maximum Likelihood Criterion for Look-Ahead Unscented Rao-Blackwellised Particle Filtering Algorithm

The likelihood for the prediction of observation at time t, $\widehat{\boldsymbol{y}}_{t|t-1}^{(i)}(z_t)$, for the i^{th} particle at time t for the discrete state z_t for the la-RBPF algorithm is defined as [5]

$$\mathcal{L}(i, z_t) = \mathcal{N}(\widehat{\boldsymbol{y}}_{t|t-1}^{(i)}(z_t), \widehat{\boldsymbol{S}}_t^{(i)}(z_t)), \tag{2}$$

where $\widehat{\boldsymbol{S}}_t^{(i)}(z_t)$ represents state covariance of observation at time t of the i^{th} particle of a possible state $z_t \in \{1, ..., n_z\}$. We define the state $z_{t,\mathtt{max}}^{(i)}$ to be the discrete state which the maximum likelihood for the i^{th} particle at time t is associated with. In order to select the maximum likelihood whereas those with smaller likelihood are suppressed but not eliminated, $\mathcal{L}(i, z_t)$ in (2) is masked with a radial basis function $\phi(z_{t,\mathtt{max}}^{(i)}) = \exp(-(z_t - z_{t,\mathtt{max}}^{(i)})^2)$ where $z_t = 1, \ldots, n_z$, and $z_{t,\mathtt{max}}^{(i)} \in \{1, ..., n_z\}$ and the masked likelihood is derived by

$$\tilde{\mathcal{L}}(i, z_t) = \phi(z_{t,\mathtt{max}}^{(i)}) \cdot \mathcal{L}(i, z_t). \tag{3}$$

3.1. The UKF Update

The UKF prediction and update operation[1] for la-URBPF at time step t and for the i^{th} particle of mode z_t is performed to get $\widehat{\boldsymbol{\mu}}_t^{(i)}(z_t)$ which represents updated estimate of state mean at time t, $\widehat{\boldsymbol{\mu}}_{t|t-1}^{(i)}(z_t)$ prediction of state mean at time t, $\widehat{\boldsymbol{\Sigma}}_t^{(i)}(z_t)$ updated state covariance at time t, $\widehat{\boldsymbol{y}}_{t|t-1}^{(i)}(z_t)$ prediction of observation at time t and $\widehat{\boldsymbol{S}}_t^{(i)}(z_t)$ state covariance at time t respectively. The required input variables are $\boldsymbol{\mu}_t^{(i)}$ which represents state mean estimate at time $t-1$, $\boldsymbol{\Sigma}_t^{(i)}$ state covariance at time $t-1$, $\boldsymbol{y}_t$ observation at time t, z_t possible discrete state at time t and $\boldsymbol{z}_{t-1}^{(i)}$ mode at time $t-1$.

The original la-URBPF algorithm needs to perform one UKF prediction and updating step for ***every*** particle for N particles and for ***every*** mode for possible n_z modes [6]. This results in a prohibitively large number of $N \times n_z$ UKF calculations for each time step t which contributes to its poor capability in terms of computational complexity [7]. In [7], the Fast la-URBPF is proposed to reduce the prohibitively large number of UKF update and prediction steps required in the original la-URBPF by using ***only*** one particle as a representative of a group of particles in the same mode to undergo n_z UKF

[1]We refer the readers to [10] for the details of UKF and and to [6] for its use in the la-URBPF algorithm.

updates for eact time step. Fast la-URBPF requires less than or at most equal to $N \times n_z$ UKF calculations for each time step t. The maximum likelihood la-URBPF algorithm is shown in Algorithm 1. Most parts of the algorithm are similar to the Fast la-URBPF algorithm [7] except for the maximum likelihood masking step which the masked maximum likelihood $\tilde{\mathcal{L}}(i, z_t)$ is introduced before computing the posterior probability of particle i at state z_t ($\widehat{Post}(i, z_t)$).

4. Simulations

A simple model of the suspension system of the K-9 rover at NASA Ames Research Center as in [6] was used in all of the simulations. The model has six discrete states ($n_z = 6$) and six continuous variables, two of which, i.e., bogey angle ($Y1$) and differential angle ($Y2$), are observable. The continuous parameters follow non-linear trajectories (trigonometric functions) in three of the discrete states and are linear in the others [6]. We investigated the proposed maximum likelihood la-URBPF algorithm performance in terms of robustness to various noise levels and in terms of computational time. We compared these two aspects with those of existing algorithms, i.e., the plain vanilla Particle Filter (PF), the Unscented Particle Filter (UPF) [11], the Unscented RBPF (URBPF) [12] and the Posterior Criterion Fast la-URBPF [7] with Minimum Prior criterion (Min.Prior-Post Fast la-URBPF) as suggested in [6] for improvement in computational time. All algorithms are examined in the same fault-related environment defined by the specified transition priors which can be used to described by a transition prior matrix as

$$\boldsymbol{P}(\boldsymbol{z}_t|\boldsymbol{z}_{t-1}) = \begin{pmatrix} 0.90 & 0.10 & 0 & 0 & 0 & 0 \\ 0.01 & 0.89 & 0 & 0 & 0.10 & 0 \\ 0.01 & 0 & 0.89 & 0 & 0 & 0.10 \\ 0.10 & 0 & 0 & 0.90 & 0 & 0 \\ 0 & 0 & 0.20 & 0 & 0.80 & 0 \\ 0 & 0 & 0 & 0.20 & 0 & 0.80 \end{pmatrix}. \tag{4}$$

The rates of diagnosis errors of all algorithms were measured at $\{1, 2, 4, 8, 16, 32, 64, 128\}$ particles. To test the robustness of algorithms to a variety of noise levels, the measurement noise variances of $Y1$ and $Y2$ (i.e., $\{\sigma^2_{Y1}, \sigma^2_{Y2}\}$) were varied from $\{2\mathrm{e}-7, 1\mathrm{e}-7\}$ to $\{0.2, 0.1\}$. The maximum a posteriori (MAP) estimate was used as a diagnosis measure for the discrete mode estimation. The difference between this MAP estimate and the real discrete mode is defined as an error which is then converted to the percentage of diagnosis error. For the Min.Prior-Post Fast la-URBPF, the minimum posterior probability $\texttt{Prior}_{\texttt{min}}$ was used to eliminate the need to compute the posterior if the prior is was below the preset value of 0.1. All experiments were performed with 100 Monte Carlo runs.

Fig. 1-Fig. 4 show the mean rates with plus-minus of one standard deviation of diagnosis errors of all algorithms for various noise levels. It is clearly shown that the proposed maximum likelihood la-URBPF algorithm offers the minimum diagnosis error rates at all noise levels. The reason for PF performs better when the noise level is increased is because the noise helps particles with low importance weights move to high probability regions. URBPF outperforms PF, UPF, Fast la-URBPF and Min.Prior-Post Fast la-URBPF if the number of particles is large ***or*** the level of noise is more aggravated. Note that at 16 particles, the maximum likelihood la-URBPF algorithm shows a sign of convergence to the minimum diagnosis error for all noise levels.

Fig. 5-Fig. 8 show the computational times to complete of all algorithms for various noise levels. Fast URBPF and Min.Prior-Post Fast la-URBPF show how they are sensitive to high noise and their computational times are increased noticeably at lower numbers of particles as in Fig. 8. The maximum likelihood la-URBPF algorithm is less sensitive to noise and needs the least time to complete its computation in all levels of noise environments.

Algorithm 1: The Maximum Likelihood la-URBPF Algorithm

for each time step t **do**
  Initialise $\mathcal{Z}_t \leftarrow \{\}$ and sample $\boldsymbol{z}_0^{(i)}$ from the prior $p(z_0)$ and sample $\boldsymbol{\mu}_0^{(i)}(z_0)$ and $\boldsymbol{\Sigma}_0^{(i)}(z_0)$.
  Unscented Kalman Prediction step:
  For $i = 1$ and for $z_t = 1, \ldots, n_z$, compute $\widehat{\boldsymbol{\mu}}_t^{(1)}(z_t)$, $\widehat{\boldsymbol{\Sigma}}_t^{(1)}(z_t)$, $\widehat{\boldsymbol{y}}_{t|t-1}^{(1)}(z_t)$, $\widehat{\boldsymbol{S}}_t^{(1)}(z_t)$ with $\boldsymbol{\mu}_t^{(1)}$,$\boldsymbol{\Sigma}_t^{(1)}$, $\boldsymbol{y}_t$ and $z_t, \boldsymbol{z}_{t-1}^{(1)}$ as inputs and $\widehat{Post}(1, z_t)$ with (2) and $\mathcal{Z}_t \leftarrow \{z_t^{(1)}\}$
  for $i = 2$ to N **do**
    Initialise $\mathcal{L}_{\texttt{max}} \leftarrow 0$.
    if $z_t^{(i)} \in \mathcal{Z}_t^{(j)}$ where $j \in \{1, \ldots, N\}$ and $j < i$ **then**
      $\widehat{\boldsymbol{\mu}}_t^{(i)}(z_t) \leftarrow \widehat{\boldsymbol{\mu}}_t^{(j)}(z_t)$, $\widehat{\boldsymbol{\Sigma}}_t^{(i)}(z_t) \leftarrow \widehat{\boldsymbol{\Sigma}}_t^{(j)}(z_t)$, $\widehat{\boldsymbol{y}}_{t|t-1}^{(i)}(z_t) \leftarrow \widehat{\boldsymbol{y}}_{t|t-1}^{(j)}(z_t)$, $\widehat{\boldsymbol{S}}_t^{(i)}(z_t) \leftarrow \widehat{\boldsymbol{S}}_t^{(j)}(z_t)$ and $\widehat{Post}(i, z_t) \leftarrow \widehat{Post}(j, z_t)$
    else
      for $z_t = 1, \ldots, n_z$ **do**
        if $\boldsymbol{P}(z_t^{(i)}, z_t) = 0$ **then**
          $\widehat{Post}(i, z_t) \leftarrow 0$
        else
          Perform the UKF update to get $\widehat{\boldsymbol{\mu}}_t^{(i)}(z_t)$, $\widehat{\boldsymbol{\Sigma}}_t^{(i)}(z_t)$, $\widehat{\boldsymbol{y}}_{t|t-1}^{(i)}(z_t)$ and $\widehat{\boldsymbol{S}}_t^{(i)}(z_t)$ with $\boldsymbol{\mu}_t^{(i)}, \boldsymbol{\Sigma}_t^{(i)}, \boldsymbol{y}_t, z_t, \boldsymbol{z}_{t-1}^{(i)}$ as inputs and $\mathcal{L}(i, z_t)$ with (2) and set $\mathcal{Z}_t \leftarrow \{\mathcal{Z}_t, z_t^{(i)}\}$
          if $\mathcal{L}_{\texttt{max}} < \mathcal{L}(i, z_t)$ **then**
            $\mathcal{L}_{\texttt{max}} \leftarrow \mathcal{L}(i, z_t)$
            $z_{t,\texttt{max}}^{(i)} \leftarrow z_t$
          end if
        end if
      end for
      Maximum Likelihood Masking step:
      Perform the Radial Basis Function on the likelihood $\mathcal{L}(i, z_t)$ centred at the maximum mode $z_{t,\texttt{max}}^{(i)}$
      $\tilde{\mathcal{L}}(i, z_t) \leftarrow \phi(z_{t,\texttt{max}}^{(i)}) \cdot \mathcal{L}(i, z_t)$. For $z_t = 1, \ldots, n_z$, calculate the posterior of particle i at mode z_t
      $\widehat{Post}(i, z_t) \leftarrow \tilde{\mathcal{L}}(i, z_t) \cdot \boldsymbol{P}(z_t^{(i)}, z_t)$ where $\boldsymbol{P}(z_t^{(i)}, z_t)$ is the transition prior from state $z_t^{(i)}$ to state z_t.
    end if
  end for
  For $i = 1, \ldots, N$, evaluate and normalise the importance weights: $w_t^{(i)} = \sum_{z_t=1}^{n_z} \widehat{Post}(i, z_t)$
  Selection Step:
  Multiply/Discard particles $\{\widehat{\boldsymbol{\mu}}_t^{(i)}, \widehat{\boldsymbol{\Sigma}}_t^{(i)}, \widehat{\boldsymbol{z}}_{t-1}^{(i)}, \widehat{Post}(i, z_t)\}_{i=1}^N$ with respect to high/low importance weights $w_t^{(i)}$ to obtain N particles $\{\boldsymbol{\mu}_t^{(i)}, \boldsymbol{\Sigma}_t^{(i)}, \boldsymbol{z}_{t-1}^{(i)}, Post(i, z_t)\}_{i=1}^N$.
  Sequential Importance Sampling Step:
  For $i = 1, ..., N$, compute

$$p(\boldsymbol{z}_t | \boldsymbol{z}_{t-1}^{(i)}, \boldsymbol{y}_{1:t}) \propto Post(i, z_t)$$

  Sampling step: $z_t^{(i)} \sim p(\boldsymbol{z}_t | \boldsymbol{z}_{t-1}^{(i)}, \boldsymbol{y}_{1:t})$
  Updating Step:
  For $i = 1, ..., N$, set $\boldsymbol{z}_t^{(i)} \leftarrow z_t^{(i)}$ and using the previously computed results in the Unscented Kalman Prediction step to acquire $\boldsymbol{\mu}_t^{(i)} \leftarrow \boldsymbol{\mu}_t^{(i)}(z_t^{(i)})$ and $\boldsymbol{\Sigma}_t^{(i)} \leftarrow \boldsymbol{\Sigma}_t^{(i)}(z_t^{(i)})$
end for

5. Conclusions

We have proposed a new maximum likelihood technique for look-ahead unscented Rao-Blackwellised particle filtering (la-URBPF) algorithm. Although la-URBPF generally outperforms URBPF in low noise environments, it struggles to perform correctly in high noise ones. By introducing the maximum likelihood technique to la-URBPF, the state with maximum likelihood is selected for computing posterior probability whereas disturbing likelihood can be masked by means of a radial basis function. Simulation results show how the maximum likelihood la-URBPF algorithm can achieve the best performance in either low or high noise levels while Fast la-URBPF performs the best out of the existing algorithms in low noise and with low numbers of particles. While in high noise, Fast la-URBPF is almost surely guaranteed to fail whereas the proposed maximum likelihood la-URBPF algorithm still maintains the best performance compared to all the existing algorithms. Unlike other fast versions of URBPF, the computation time of the proposed algorithm is less sensitive to noise and hence suggests its applicability in time-critical or in resource-restricted embedded systems.

References

[1] R. Dearden and D. Clancy, "Particle filters for real-time fault detection in planetary rovers," in ***Proceedings of the Thirteenth International Workshop on Principles of Diagnosis***, Semmering, Austria, 2002, pp. 1–6.

[2] V. Verma, G. Gordon, R. Simmons, and S. Thrun, "Real-time fault diagnosis," ***Robotics & Automation Magazine***, vol. 11, no. 2, pp. 56–66, 2004.

[3] R. Morales-menéndez, N. D. Freitas, and D. Poole, "Real-time monitoring of complex industrial processes with particle filters," in ***Neural Information Processing Systems***, 2002, pp. 1433–1440.

[4] M. Lin, R. Chen, and J. S. Liu, "Lookahead strategies for sequential monte carlo," ***Statistical Science***, vol. 28, no. 1, pp. 69–94, 2013.

[5] N. De Freitas, R. Dearden, F. Hutter, R. Morales-menéndez, J. Mutch, and D. Poole, "Diagnosis by a waiter and a mars explorer," ***In Invited paper for Proceedings of the IEEE, special***, vol. 92, no. 3, pp. 455–468, 2004.

[6] F. Hutter and R. Dearden, "Efficient on-line fault diagnosis for non-linear systems," in ***Proceedings of the Seventh International Symposium on Artificial Intelligence and Robotics in Space (i-SAIRAS-03)***, 2003.

[7] P. Yuvapoositanon, "Fast computation of look-ahead unscented rao-blackwellised particle filters," in ***Proceedings of the Electrical Engineering/Electronics, Computer, Telecommunications and Information Technology (ECTI-CON)***, Cha-Am, Petchburi, Thailand, 2012.

[8] ——, "Fast computation of look-ahead rao-blackwellised particle filter in SLAM," in ***Proceedings of the International Electrical Engineering Congress 2014***, Pattaya, Chonburi, Thailand, 2014.

[9] J. L. F. Quintanilla, J. P. N. González, R. Morales-Menéndez, and R. Ramírez, "A monitoring and diagnosis system for electric machines based on bayesian networks," in ***Asociación Mexicana de Control Automático (AMC2004)***, Mexico, 2004.

[10] S. J. Julier and J. K. Uhlmann, "Unscented filtering and nonlinear estimation," in ***Proceedings of the IEEE***, 2004, pp. 401–422.

[11] R. van der Merwe, A. Doucet, N. de Freitas, and E. A. Wan, "The unscented particle filter," in ***Neural Information Processing Systems (NIPS)***, Denver, CO, USA, 2000, pp. 584–590.

[12] F. Hutter, R. Dearden, T. U. Darmstadt, and F. Informatik, "The gaussian particle filter for diagnosis of non-linear systems," in ***Proceedings of the 14th International Conference on Principles of Diagnosis(DX03)***, 2003, pp. 65–70.

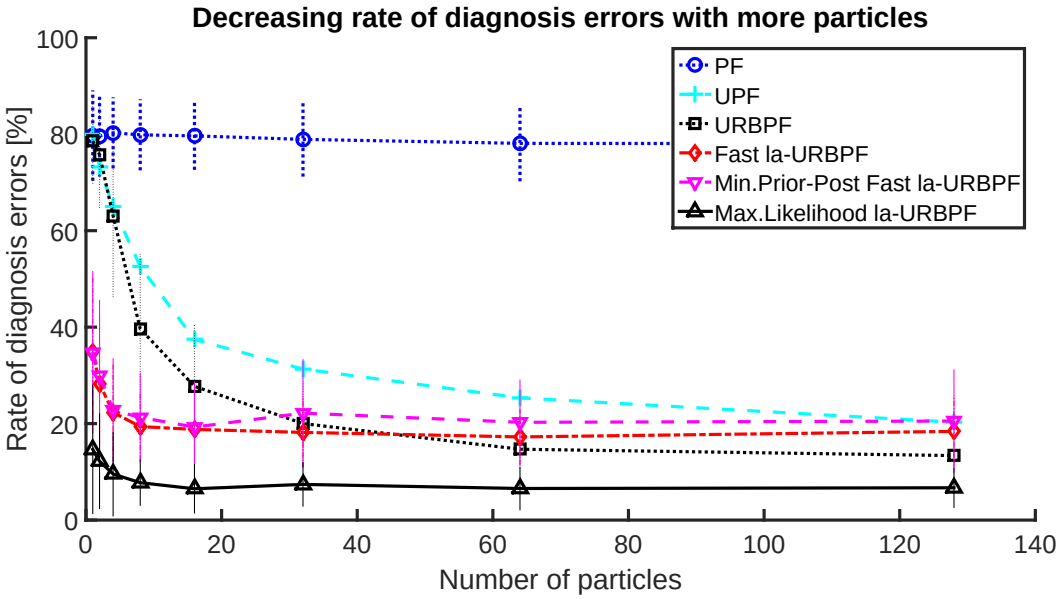

Fig. 1. Diagnosis Errors for $\{\sigma^2_{Y1}, \sigma^2_{Y2}\} = \{2\mathrm{e}-7, 1\mathrm{e}-7\}$.

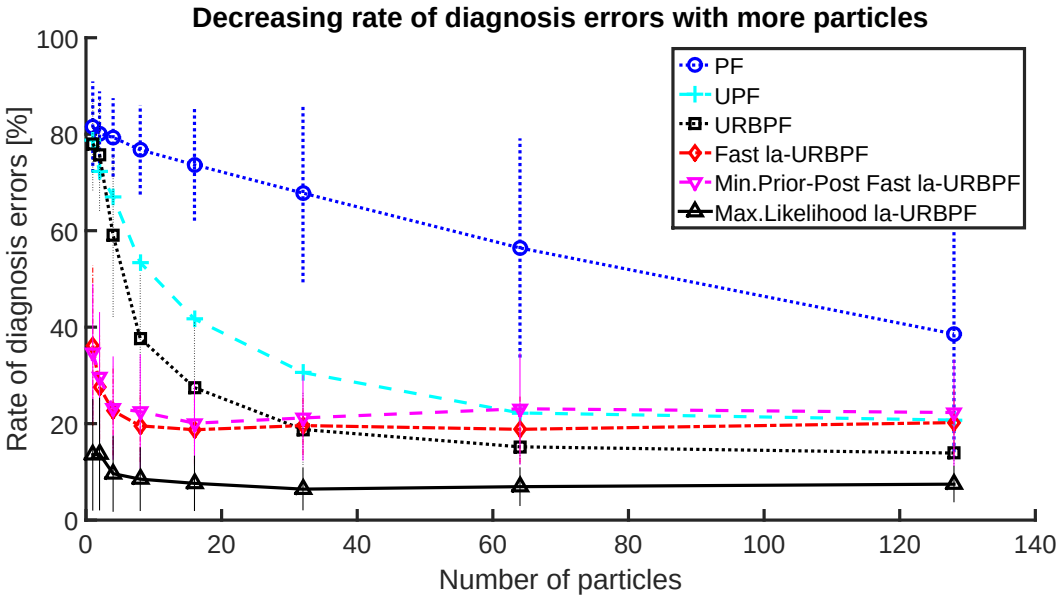

Fig. 2. Diagnosis Errors for $\{\sigma^2_{Y1}, \sigma^2_{Y2}\} = \{2\mathrm{e}-5, 1\mathrm{e}-5\}$.

DOI:10.4186/ej.2017.21.6.47

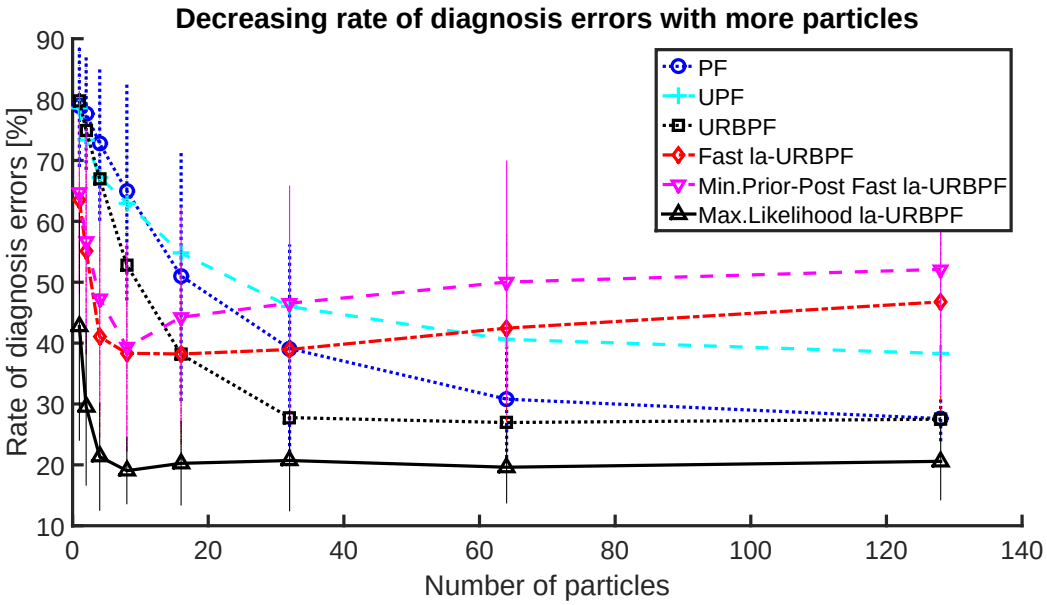

Fig. 3. Diagnosis Errors for $\{\sigma^2_{Y1}, \sigma^2_{Y2}\} = \{2\mathrm{e}-3, 1\mathrm{e}-3\}$.

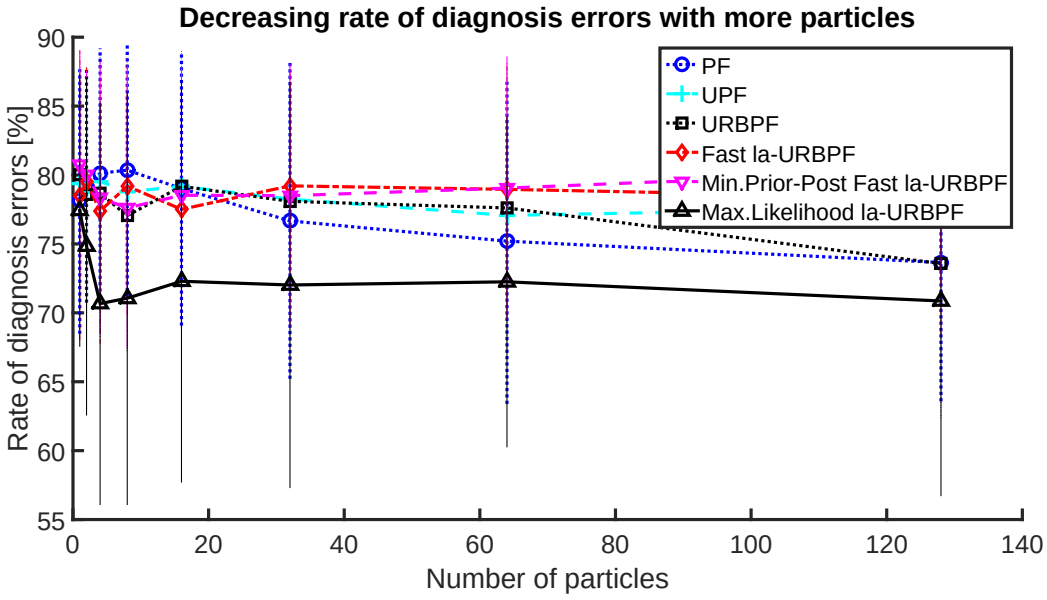

Fig. 4. Diagnosis Errors for $\{\sigma^2_{Y1}, \sigma^2_{Y2}\} = \{2\mathrm{e}-1, 1\mathrm{e}-1\}$.

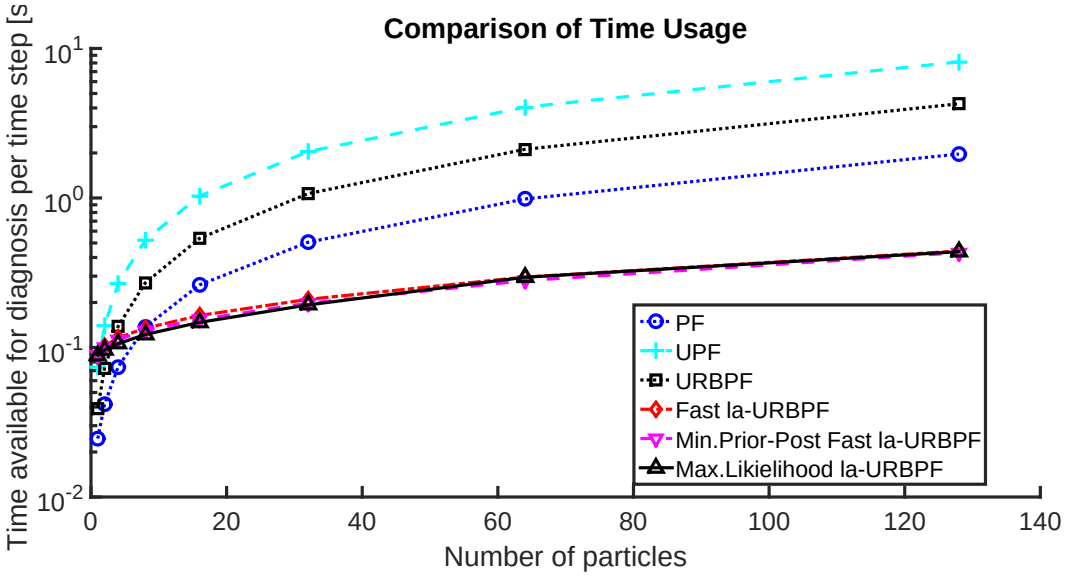

Fig. 5. Computational Time for $\{\sigma_{Y1}^2, \sigma_{Y2}^2\} = \{2\mathrm{e}-7, 1\mathrm{e}-7\}$.

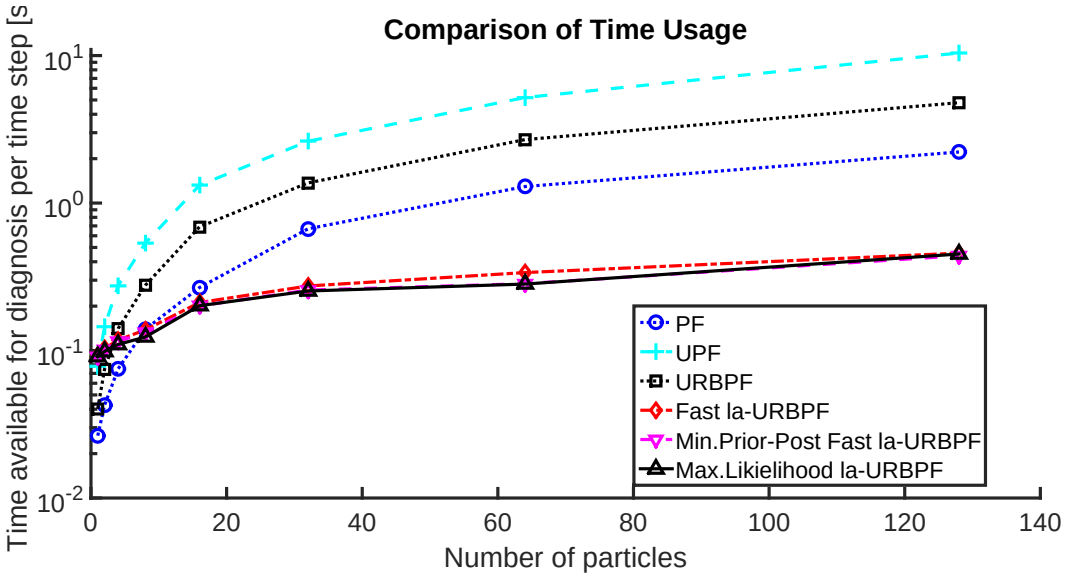

Fig. 6. Computational Time for $\{\sigma_{Y1}^2, \sigma_{Y2}^2\} = \{2\mathrm{e}-5, 1\mathrm{e}-5\}$.

DOI:10.4186/ej.2017.21.6.47

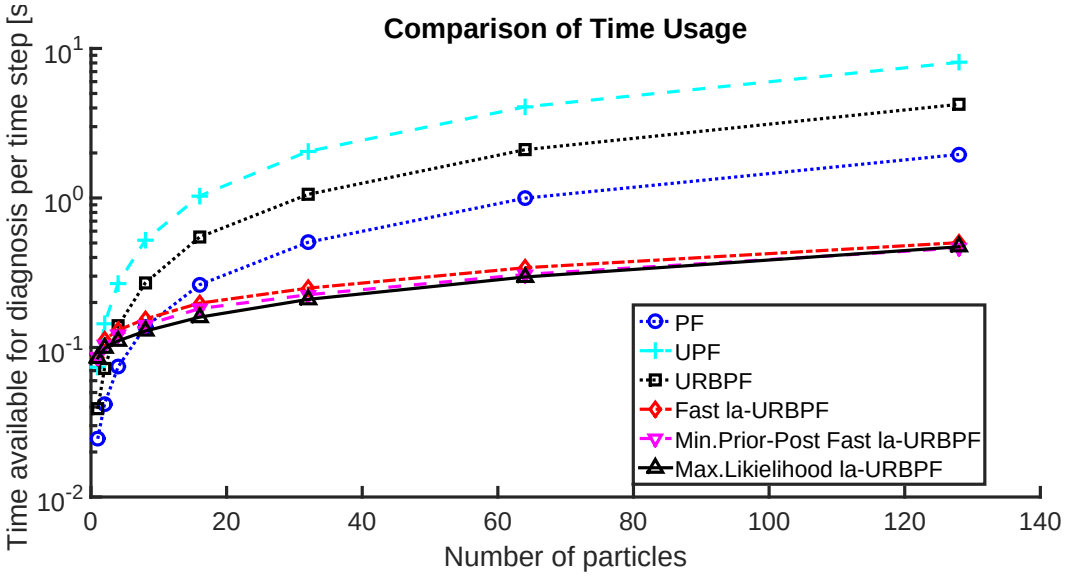

Fig. 7. Computational Time for $\{\sigma_{Y1}^2, \sigma_{Y2}^2\} = \{2\mathrm{e}-3, 1\mathrm{e}-3\}$.

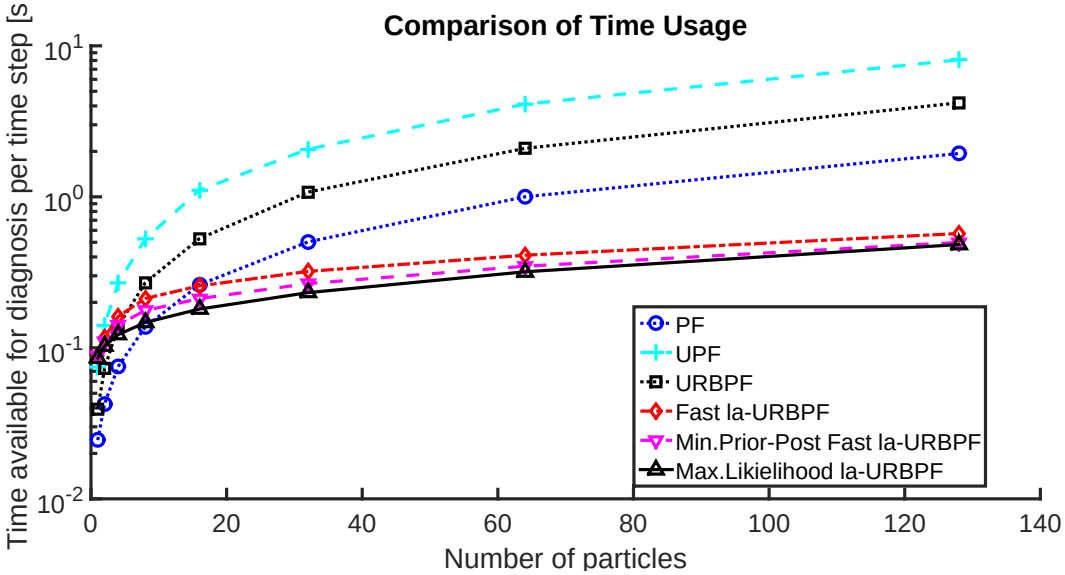

Fig. 8. Computational Time for $\{\sigma_{Y1}^2, \sigma_{Y2}^2\} = \{2\mathrm{e}-1, 1\mathrm{e}-1\}$.